

Three-body models of electron-hydrogen ionization

S. Jones and D. H. Madison

Physics Department, University of Missouri-Rolla, Rolla, Missouri 65401

D. A. Kononov

Electronic Structure of Materials Centre, The Flinders University of South Australia, G.P.O. Box 2100, Adelaide, SA 5001, Australia

(Received 24 June 1996; revised manuscript received 23 September 1996)

In this paper, we report calculations of electron-hydrogen ionization whereby the final-state wave function is approximated by recently reported analytical three-body wave functions. In a first model we use the wave function of Alt and Mukhamedzhanov [Phys. Rev. A **47**, 2004 (1993)], and in a second model we use the wave function of Berakdar [Phys. Rev. A **53**, 2314 (1996)]. [S1050-2947(97)08701-5]

PACS number(s): 34.80.Dp, 34.10.+x, 03.65.Nk

I. INTRODUCTION

In recent years, significant progress has been made in the theoretical treatment of atomic ionization by electron impact—the ($e, 2e$) problem. Following the work of Brauner, Briggs, and Klar [1], considerable attention has been given to using final-state wave functions in theoretical calculations that asymptotically satisfy the three-body Schrödinger equation. The wave functions used in these “three-body” models depend explicitly on the electron-electron separation and as a result are significantly more difficult to use in a practical calculation than “two-body” wave functions, which depend only upon electron-nucleus separations. On the other hand, the three-body wave functions represented an important advancement in that they explicitly contain the Coulomb interaction between the two electrons to all orders of perturbation theory while this interaction is only contained to first order in a first-order perturbation theory calculation.

In this work, we study electron-hydrogen ionization using two analytical three-body wave functions recently reported in the literature. To this end, we have written a computer program that performs the necessary integration for the scattering amplitude by direct, six-dimensional numerical quadrature. This method is surprisingly efficient for a judicious choice of coordinate system, as will be explained below. In Sec. II, general theory is discussed, followed by a detailed presentation of the two models. Our numerical method is discussed in Sec. III. In Sec. IV, our results are presented and discussed, followed by our conclusions in Sec. V. Atomic units (a.u.) are used throughout this work and unit vectors are denoted by a “hat,” e.g., $\hat{\mathbf{r}} = \mathbf{r}/r$. The reduced mass of two electrons is denoted by $\mu = 1/2$. We ignore corrections of order m_e/m_p , where m_e is the electron mass and m_p is the proton mass.

II. THEORY

Consider an incident electron with wave vector \mathbf{k}_i ionizing atomic hydrogen. In the final state, electrons with wave vectors \mathbf{k}_a and \mathbf{k}_b emerge (with relative wave vector $\mathbf{k}_{ab} = \mu[\mathbf{k}_a - \mathbf{k}_b]$). The triply differential cross section (TDCS) for this process is given by

$$\frac{d^3\sigma}{d\Omega_a d\Omega_b dE_b} = \frac{k_a k_b}{k_i} [|f|^2 + |g|^2 + |f-g|^2] / 2, \quad (1)$$

where

$$f = -(2\pi)^{-5/2} \langle \Psi_f^- | V_i | \beta_i \rangle \quad (2)$$

is the direct amplitude and g is the exchange amplitude, which may be obtained from Eq. (2) by exchanging the roles of the two electrons in the nonantisymmetrized final-state wave function Ψ_f^- . Here

$$\beta_i = e^{i\mathbf{k}_i \cdot \mathbf{r}_a} \psi_i(\mathbf{r}_b) \quad (3)$$

is the unperturbed initial state and the perturbation

$$V_i = -\frac{1}{r_a} + \frac{1}{r_{ab}} \quad (4)$$

is the interaction between the incident electron and the atom, with \mathbf{r}_a and \mathbf{r}_b the coordinates of the two electrons relative to the nucleus, $\mathbf{r}_{ab} = \mathbf{r}_a - \mathbf{r}_b$ their relative coordinate, and $\psi_i(\mathbf{r}_b) = e^{-r_b/\sqrt{\pi}}$ the ground-state orbital for the hydrogen atom.

The exact scattering wave function for the system, developed from the final asymptotic state and with prescribed incoming flux, is a solution of

$$(H - E)\Psi_f^- = 0, \quad (5)$$

where

$$E = \frac{1}{2}k_a^2 + \frac{1}{2}k_b^2 \quad (6)$$

is the total energy and

$$H = -\frac{1}{2}\nabla_{\mathbf{r}_a}^2 - \frac{1}{2}\nabla_{\mathbf{r}_b}^2 - \frac{1}{r_a} - \frac{1}{r_b} + \frac{1}{r_{ab}} \quad (7)$$

is the full Hamiltonian.

Figure 1 shows a simple schematic representation of the various asymptotic regions. In this figure, the radial coordinate of the incident electron is r_a , and that for the atomic

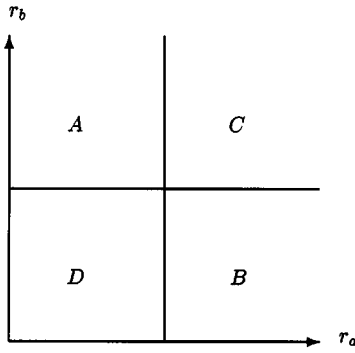


FIG. 1. Schematic representation of asymptotic regions, as described in the text.

electron is r_b . In region D , both r_a and r_b are finite, whereas in region C , both are infinite. In region B , r_b is finite but r_a is infinite and in region A , r_a is finite but r_b is infinite. From Eq. (3), it is seen that only finite values of r_b can contribute to the scattering amplitude since this coordinate is for an electron that was initially bound. Consequently, regions A and C do not contribute to the scattering amplitude, Eq. (2). Furthermore, as can be seen from Eq. (4), region B does not contribute to the amplitude either, since a multipole expansion of $1/r_{ab}$ reveals that the perturbation V_i vanishes there as $1/r_a^2$. As a result, only region D contributes to scattering. Although the asymptotic regions do not contribute to scattering amplitudes, the behavior in the asymptotic regions governs the form of the wave function in region D , and thus strongly influences the results of a scattering calculation.

We now turn our attention to some of the approximations for Ψ_f^- made in the past. Bethe [2], using the first-Born approximation in 1930, performed the first quantum-mechanical calculation for atomic ionization. In the first-Born approximation for electron-hydrogen ionization, the final-state wave function is approximated by the product of a plane wave for the scattered electron and a Coulomb wave for the ejected electron (a two-body wave function):

$$\Psi_{f,B1}^- = e^{i(\mathbf{k}_a \cdot \mathbf{r}_a + \mathbf{k}_b \cdot \mathbf{r}_b)} C(-1/k_b, \mathbf{k}_b, \mathbf{r}_b). \quad (8)$$

Here

$$C(\alpha, \mathbf{k}, \mathbf{r}) = \Gamma(1 - i\alpha) e^{-(\pi/2)\alpha} F(i\alpha, 1; -i(kr + \mathbf{k} \cdot \mathbf{r})) \quad (9)$$

is a Coulombic distortion factor with Γ the gamma function and F the confluent hypergeometric function. Substituting this wave function into the Schrödinger equation, we obtain

$$(H - E)\Psi_{f,B1}^- = W_{f,B1}^- \Psi_{f,B1}^-, \quad (10)$$

where we have defined a *perturbing energy*

$$W_{f,B1}^- = -\frac{1}{r_a} + \frac{1}{r_{ab}}. \quad (11)$$

We see from Eq. (11) that the perturbing energy $W_{f,B1}^-$ vanishes as $1/r_a^2$ when r_a tends to infinity for finite r_b . As a result, $\Psi_{f,B1}^-$ is an asymptotic solution of the Schrödinger equation in region B of Fig. 1. This wave function, however,

does not satisfy the asymptotic boundary condition when all interparticle separations tend to infinity, nor is it correct for $r_b \rightarrow \infty, r_a/r_b \rightarrow 0$ (region A).

Redmond [3], ca. 1972, as cited in Rosenberg [4], discovered the asymptotic form for three charged particles in the continuum valid when all interparticle separations tend to infinity. For two continuum electrons in the field of a proton, it is given by

$$\tilde{\Psi}_f^- = e^{i(\mathbf{k}_a \cdot \mathbf{r}_a + \mathbf{k}_b \cdot \mathbf{r}_b)} e^{i\phi}, \quad (12)$$

where

$$\begin{aligned} \phi = & \frac{1}{k_a} \ln(k_a r_a + \mathbf{k}_a \cdot \mathbf{r}_a) + \frac{1}{k_b} \ln(k_b r_b + \mathbf{k}_b \cdot \mathbf{r}_b) \\ & - \frac{\mu}{k_{ab}} \ln(k_{ab} r_{ab} + \mathbf{k}_{ab} \cdot \mathbf{r}_{ab}). \end{aligned} \quad (13)$$

Substituting this wave function into the Schrödinger equation yields a perturbing energy [5]

$$\begin{aligned} \tilde{W}_f^- = & \mu \frac{\hat{\mathbf{k}}_{ab} + \hat{\mathbf{r}}_{ab}}{k_{ab} r_{ab} + \mathbf{k}_{ab} \cdot \mathbf{r}_{ab}} \cdot \left[\frac{\hat{\mathbf{k}}_a + \hat{\mathbf{r}}_a}{k_a r_a + \mathbf{k}_a \cdot \mathbf{r}_a} - \frac{\hat{\mathbf{k}}_b + \hat{\mathbf{r}}_b}{k_b r_b + \mathbf{k}_b \cdot \mathbf{r}_b} \right] \\ & + \frac{1}{k_a r_a (k_a r_a + \mathbf{k}_a \cdot \mathbf{r}_a)} + \frac{1}{k_b r_b (k_b r_b + \mathbf{k}_b \cdot \mathbf{r}_b)} \\ & + \frac{2\mu^2}{k_{ab} r_{ab} (k_{ab} r_{ab} + \mathbf{k}_{ab} \cdot \mathbf{r}_{ab})}. \end{aligned} \quad (14)$$

Redmond's form is valid in region C of Fig. 1, provided $r_{ab} \rightarrow \infty$ (to simplify the presentation, the electron-electron separation, r_{ab} , is not shown in Fig. 1). It may be seen from Eq. (14) that Redmond's form is not valid if only *one* of the escaping electrons is far from the ion (regions A and B), or if both electrons are far from the ion but not far from each other. Brauner, Briggs, and Klar [1] performed calculations for electron-hydrogen ionization using the "3C" final-state wave function,

$$\begin{aligned} \Psi_{f,3C}^- = & e^{i(\mathbf{k}_a \cdot \mathbf{r}_a + \mathbf{k}_b \cdot \mathbf{r}_b)} C(-1/k_a, \mathbf{k}_a, \mathbf{r}_a) \\ & \times C(-1/k_b, \mathbf{k}_b, \mathbf{r}_b) C(\mu/k_{ab}, \mathbf{k}_{ab}, \mathbf{r}_{ab}), \end{aligned} \quad (15)$$

which reduces to Redmond's asymptotic form in the limit that all interparticle separations tend to infinity.

Recently, Alt and Mukhamedzhanov [6], hereafter referred to as AM, derived *in closed form* a wave function for three charged particles in the continuum that is asymptotically correct in *all* asymptotic domains (regions A , B , and C of Fig. 1); that is, a wave function valid provided *at least one* electron is far from the ion regardless of the separation between the two electrons. The regions of validity for the AM wave function *enclose* the scattering region (region D of Fig. 1), and thus the AM wave function represents the proper boundary condition for this three-body problem. Berakdar [7], using a different approach, proposed a "DS3C" (dynamic screening 3C) approximate analytical solution of the Schrödinger equation for two electrons in the field of a proton. The AM and DS3C wave functions are discussed in detail below.

A. AM model

The AM wave function, as previously noted, satisfies the final-state boundary condition in all asymptotic domains (regions A , B , and C of Fig. 1). It is given by

$$\Psi_{f,AM}^- = e^{i(\mathbf{k}_a \cdot \mathbf{r}_a + \mathbf{k}_b \cdot \mathbf{r}_b)} C(-1/k'_a, \mathbf{k}'_a, \mathbf{r}_a) \times C(-1/k'_b, \mathbf{k}'_b, \mathbf{r}_b) C(\mu/k'_{ab}, \mathbf{k}'_{ab}, \mathbf{r}_{ab}). \quad (16)$$

The novel feature of this wave function is that the electrons do not have fixed wave vectors. Rather, in each Coulomb distortion factor, *local* wave vectors are required as follows.

$$\mathbf{k}'_a = \mathbf{k}_a + \mathbf{K}(\mu/k_{ba}, \mathbf{k}_{ba}, \mathbf{r}_b), \quad (17a)$$

$$\mathbf{k}'_b = \mathbf{k}_b + \mathbf{K}(\mu/k_{ab}, \mathbf{k}_{ab}, \mathbf{r}_a), \quad (17b)$$

$$\mathbf{k}'_{ab} = \mathbf{k}_{ab} + \mathbf{K}(-1/k_a, \mathbf{k}_a, \boldsymbol{\rho}) - \mathbf{K}(-1/k_b, \mathbf{k}_b, \boldsymbol{\rho}). \quad (17c)$$

Here $\boldsymbol{\rho} = \mu(\mathbf{r}_a + \mathbf{r}_b)$ is the coordinate for the center of mass of the two electrons and

$$\mathbf{K}(\eta, \mathbf{k}, \mathbf{r}) = \frac{r}{R} \left[\frac{F(1+i\eta, 2; -i(kr + \mathbf{k} \cdot \mathbf{r}))}{-iF(i\eta, 1; -i(kr + \mathbf{k} \cdot \mathbf{r}))} \right] (\hat{\mathbf{k}} + \hat{\mathbf{r}}) \quad (18)$$

is a local modification of the wave vector with $R = r_a + r_b + r_{ab}$ the ‘‘size’’ of the triangle formed by the three particles. The asymptotic form of $\Psi_{f,AM}^-$ is valid in all asymptotic domains and may be obtained [6] by replacing \mathbf{K} with

$$\mathbf{K}_{asy}(\mathbf{k}, \mathbf{r}) = \frac{\hat{\mathbf{k}} + \hat{\mathbf{r}}}{kR(1 + \hat{\mathbf{k}} \cdot \hat{\mathbf{r}})} \quad (19)$$

in Eq. (18). Note that while \mathbf{K} is a *complex* vector function, \mathbf{K}_{asy} is real. Since only the real part of \mathbf{K} is needed to satisfy the boundary condition, we have neglected the imaginary part of \mathbf{K} in the present work.

The above wave function, $\Psi_{f,AM}^-$, is an exact asymptotic solution of the Schrödinger equation for $r_a \rightarrow \infty$ and/or $r_b \rightarrow \infty$, i.e., it is an asymptotic solution *everywhere* outside the closed and finite region D of Fig. 1. In contrast, the 3C wave function, Eq. (15), which may be obtained from $\Psi_{f,AM}^-$ by neglecting \mathbf{K} in Eq. (17), is asymptotically correct only if r_a , r_b , and r_{ab} *all* become infinitely large. This same deficiency is present in later approximations [8,9], which introduced purely short-range two-body effects into the Redmond wave function.

B. DS3C model

Berakdar [7] showed that the Schrödinger equation is *invariant* under a transformation to local charges $z_a(\mathbf{r}_a, \mathbf{r}_b)$, $z_b(\mathbf{r}_a, \mathbf{r}_b)$, $z_{ab}(\mathbf{r}_a, \mathbf{r}_b)$, satisfying

$$-\frac{z_a}{r_a} - \frac{z_b}{r_b} - \frac{z_{ab}}{r_{ab}} = -\frac{1}{r_a} - \frac{1}{r_b} + \frac{1}{r_{ab}}. \quad (20)$$

This observation can be used to improve three-body wave functions. In particular, Berakdar [7] proposed the DS3C

(dynamic screening 3C) wave function (here we have normalized Berakdar’s unnormalized wave function to the asymptotic flux $\mathbf{k}_a + \mathbf{k}_b$),

$$\Psi_{f,DS3C}^- = e^{i(\mathbf{k}_a \cdot \mathbf{r}_a + \mathbf{k}_b \cdot \mathbf{r}_b)} C(-z_a/k_a, \mathbf{k}_a, \mathbf{r}_a) \times C(-z_b/k_b, \mathbf{k}_b, \mathbf{r}_b) C(-z_{ab}\mu/k_{ab}, \mathbf{k}_{ab}, \mathbf{r}_{ab}), \quad (21)$$

with charges

$$z_a = 1 - Z(\mathbf{r}_a, \mathbf{r}_b), \quad (22a)$$

$$z_b = 1 - Z(\mathbf{r}_b, \mathbf{r}_a), \quad (22b)$$

$$z_{ab} = -1 + Z(\mathbf{r}_a, \mathbf{r}_b)r_{ab}/r_a + Z(\mathbf{r}_b, \mathbf{r}_a)r_{ab}/r_b, \quad (22c)$$

as an approximate analytical solution of the Schrödinger equation. Here

$$Z(\mathbf{r}_a, \mathbf{r}_b) = \left[\frac{3 + \cos^2[4\alpha(r_b)]}{4} \right]^2 \frac{r_{ab}r_a^2}{(r_a + r_b)^3} \quad (23)$$

is a local screening of the nuclear charge with $\alpha(r) = \cos^{-1}(r/\sqrt{r_a^2 + r_b^2})$. It should be noted that there was a topographical error in the original publication which has been corrected here. It is readily seen that the charges represented by Eq. (22) satisfy the condition for invariance, Eq. (20). The particular ansatz for the charge Z , Eq. (23), was made by Berakdar [7] for the purpose of both satisfying boundary conditions as well as giving the proper behavior on the Wannier [10] ridge ($\mathbf{r}_b = -\mathbf{r}_a$). As a result, this a wave function designed to incorporate some proper physics of the nonasymptotic region D . We are especially interested in studying this model for the Wannier kinematic ($\mathbf{k}_b = -\mathbf{k}_a$) for *near-threshold* energies. This will be considered in Sec. IV.

III. METHOD OF CALCULATION

We have evaluated the scattering amplitude, Eq. (2), with Ψ_f^- approximated by $\Psi_{f,AM}^-$, Eq. (16), or $\Psi_{f,DS3C}^-$, Eq. (21), using six-dimensional numerical quadrature over \mathbf{r}_a and \mathbf{r}_b . Our numerical uncertainty is less than 5%. The integration over \mathbf{r}_b is performed first, so that the use of convergence factors may be avoided. This numerical method is efficient (about five minutes on a workstation to compute one scattering amplitude) if the z axis is taken along $\mathbf{q} = \mathbf{k}_i - \mathbf{k}_{a(b)}$ for the direct (exchange) amplitude and *cylindrical* coordinates are used for \mathbf{r}_a . This choice reduces the necessary computational effort by *orders of magnitude* compared to the choice of spherical coordinates with the z axis along the beam direction, since the dominant feature of the \mathbf{r}_a contribution to the scattering amplitude is $e^{i\mathbf{q} \cdot \mathbf{r}_a}$ and these three-dimensional oscillations are treated in one dimension with the above choice of coordinate system.

IV. RESULTS

In Fig. 2, we compare our results for an incident energy of 150 eV with the absolute ($\pm 15\%$), coplaner asymmetric, experimental data of Ehrhardt *et al.* [11], and with the 3C

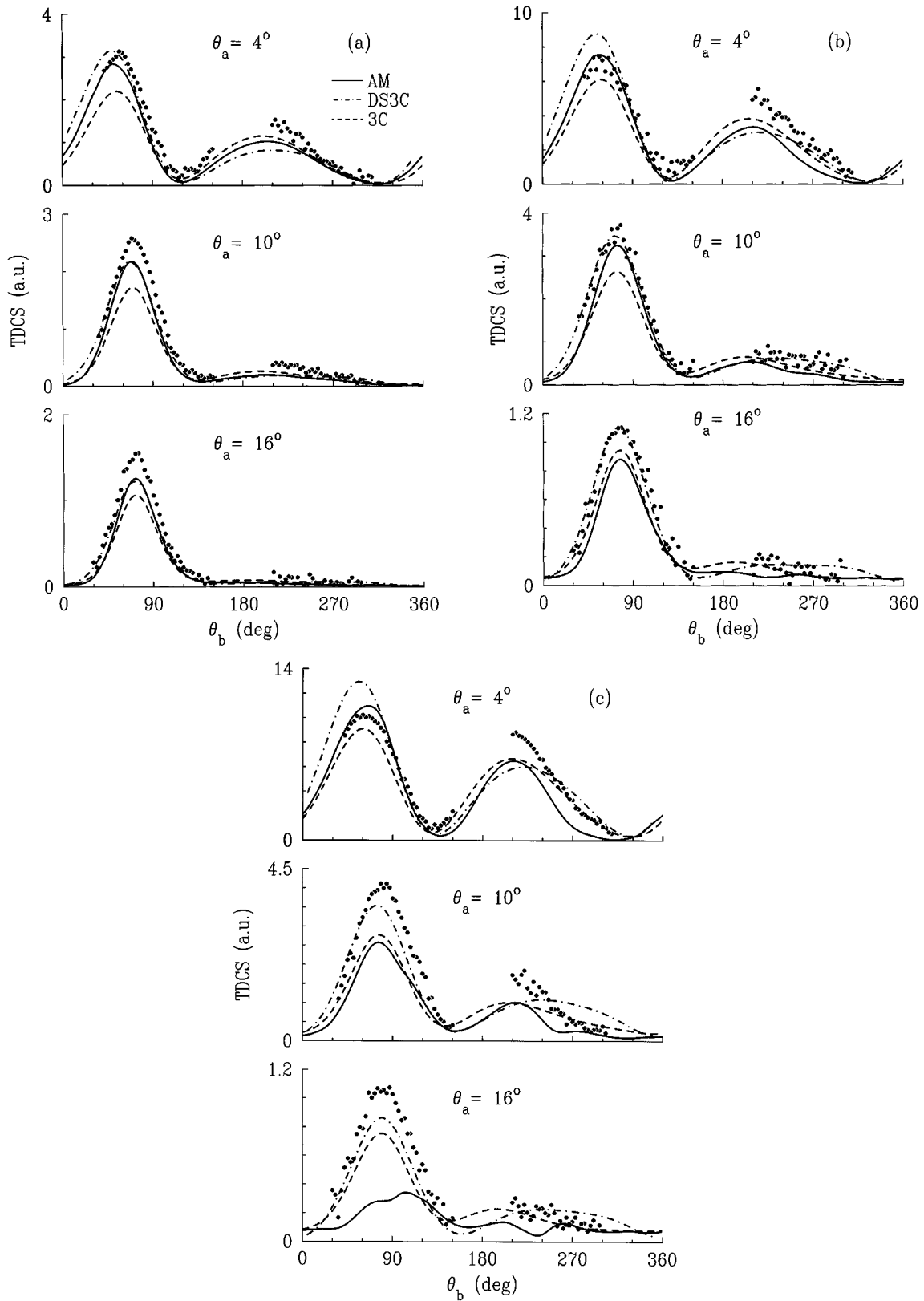


FIG. 2. Triply differential cross sections for 150-eV electron-impact ionization of hydrogen vs the angle θ_b of the ejected electron, with the angle θ_a of the scattered electron fixed as indicated. The energy of the ejected electron is (a) 10 eV, (b) 5 eV, or (c) 3 eV.

model [1]. For asymmetric kinematics, the exchange contribution is small, and so is not included. We adopt the convention that the angle of observation for the scattered electron is measured counterclockwise from the forward beam direction, while that for the ejected electron is measured

clockwise. For the case where the ejected electron has an energy of 10 eV, the AM and DS3C models are in better agreement with experiment than the 3C model. The large peak at small scattering angles is normally referred to as the binary peak and the corrections to the wave vectors (AM), or

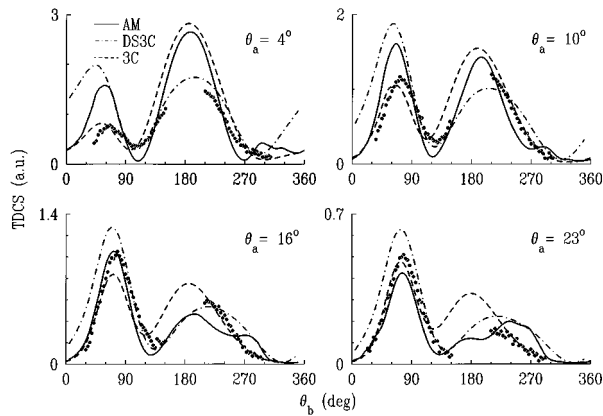


FIG. 3. Same as Fig. 2 for 54.4-eV incident energy and an ejected-electron energy of 5 eV.

to the charges (DS3C), produce a larger binary peak, in better accord with experiment, than that predicted by 3C. For an ejected-electron energy of 5 eV, the DS3C is in excellent agreement with experiment for $\theta_a = 10^\circ$ and 16° , but does not do as well for the smallest momentum transfer case (4°). The AM model, on the other hand, does well for 4° and 10° , but not as well for the largest momentum transfer case (16°). This situation for the AM model becomes much worse for the lowest ejected-electron energy (3 eV), where the model fails completely for $\theta_a = 16^\circ$. Although the shape of the AM curve for 16° would suggest that we have numerical errors, we have verified that these results are numerically converged and stable. For hard collisions (i.e., large θ_a), a wave function that is accurate for small interparticle separations is needed, and therefore the above results indicate that the AM wave function is a poor approximation for small separations (at least for small ejection energies).

Fig. 3 displays the comparison between experiment and theory for the lower energy of 54.4 eV. The experimental data of Schlemmer *et al.* [12], recently put on an absolute scale by Röder *et al.* [13], are shown. The uncertainty in the experimental normalization is approximately 35%. Here the AM results display unusual behavior for the recoil peak at the larger momentum transfers ($\theta_a = 16^\circ$ and 23°), while the DS3C results are poorest for the smallest momentum transfer case ($\theta_a = 4^\circ$), predicting a much too broad binary peak.

Finally, in Fig. 4, we consider an equal-energy near-threshold case where the two electrons leave the ion in opposite directions (Wannier kinematic). The exchange amplitude is included in these results. The experimental data of Schlemmer *et al.* [14], also recently put on an absolute scale ($\pm 22\%$) by Röder *et al.* [13], are shown. It is seen that the absolute values of the DS3C results are off by an order of magnitude (although better than that predicted by 3C), and that the agreement in shape is poor. This demonstrates that

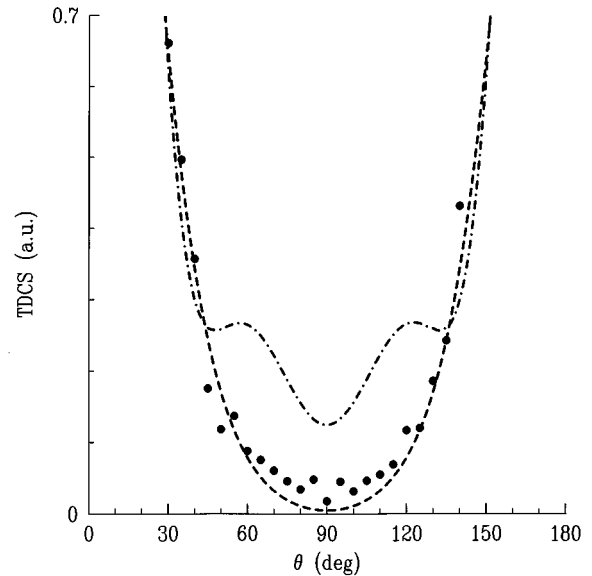


FIG. 4. Triply differential cross sections for electron-impact ionization of hydrogen, 4 eV above threshold, with equal energies for the two final-state electrons and with the angle between the two electrons fixed at 180° vs the angle θ between the interelectronic line and the beam direction. The dot-dashed line is the DS3C result (multiplied by 10.5) and the dashed line is the 3C result (multiplied by 27).

more work is required if three-body wave functions are to be reliable for near-threshold energies.

V. CONCLUSION

In this work, we reported calculations of electron-hydrogen ionization using three-body wave functions as approximations for the exact final-state wave function. Although these models sometimes failed, we believe this type of approach is very promising. It is not surprising that using a wave function that is only asymptotically correct (AM model) to represent the physics in the nonasymptotic region D can lead to poor results for some kinematics. Our results indicate that both the AM and DS3C models are high-energy approximations, with the AM model valid for small momentum transfer collisions, whereas the DS3C model is better for large momentum transfer collisions. Furthermore, it appears possible to use the ideas of Berakdar to improve the behavior of the AM wave function for small interparticle separations and this will be the direction of future work.

ACKNOWLEDGMENTS

Helpful discussions with P. L. Altick, J. Berakdar, V. Kravtsov, A. M. Mukhamedzhanov, and J. L. Peacher are gratefully acknowledged. This work was sponsored by the NSF.

[1] M. Brauner, J. S. Briggs, and H. Klar, *J. Phys. B* **22**, 2265 (1989).

[2] H. Bethe, *Ann. Phys.* **5**, 325 (1930).

[3] P. J. Redmond (unpublished).

[4] L. Rosenberg, *Phys. Rev. D* **8**, 1833 (1973).

[5] S. Jones and D. H. Madison, *J. Phys. B* **27**, 1423 (1994).

[6] E. O. Alt and A. M. Mukhamedzhanov, *Phys. Rev. A* **47**, 2004 (1993).

- [7] J. Berakdar, Phys. Rev. A **53**, 2314 (1996).
- [8] A. Franz and P. L. Altick, J. Phys. B **25**, 1577 (1992).
- [9] S. Jones, D. H. Madison, A. Franz, and P. L. Altick, Phys. Rev. A **48**, R22 (1993).
- [10] G. H. Wannier, Phys. Rev. **90**, 817 (1953).
- [11] H. Ehrhardt, K. Jung, G. Knoth, and P. Schlemmer, Z. Phys. D **1**, 3 (1986).
- [12] P. Schlemmer, T. Rösler, K. Jung, and H. Ehrhardt, J. Phys. B **22**, 2179 (1989).
- [13] J. Röder (private communication).
- [14] P. Schlemmer, T. Rösler, K. Jung, and H. Ehrhardt, Phys. Rev. Lett. **63**, 252 (1989).